Water Research 241 (2023) 120146

Contents lists available at ScienceDirect

Water Research

journal homepage: www.elsevier.com/locate/watres

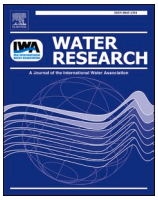

The abiotic removal of organic micropollutants with iron and manganese oxides in rapid sand filters for groundwater treatment

Jinsong Wang [a,1], David de Ridder [b], Nora B. Sutton [a,*], Baptiste A.J. Poursat [a,2], Pradip Saha [a,3], Albert van der Wal [a,b]

[a] Environmental Technology, Wageningen University & Research, P.O. Box 17, Wageningen 6700 AA, the Netherlands
[b] Evides Water Company N.V., Schaardijk 150, Rotterdam 3063 NH, the Netherlands

ARTICLE INFO

Keywords:
Organic micropollutants
Iron and manganese oxides
Rapid sand filters
Adsorption
Oxidation
Water treatment

ABSTRACT

Rapid sand filters (RSFs) have shown potential for removing organic micropollutants (OMPs) from groundwater. However, the abiotic removal mechanisms are not well understood. In this study, we collect sand from two field RSFs that are operated in series. The sand from the primary filter abiotically removes 87.5% of salicylic acid, 81.4% of paracetamol, and 80.2% of benzotriazole, while the sand from the secondary filter only removes paracetamol (84.6%). The field collected sand is coated by a blend of iron oxides (FeOx) and manganese oxides (MnOx) combined with organic matter, phosphate, and calcium. FeOx adsorbs salicylic acid via bonding of carboxyl group with FeOx. The desorption of salicylic acid from field sand indicates that salicylic acid is not oxidized by FeOx. MnOx adsorbs paracetamol through electrostatic interactions, and further transforms it into *p*-benzoquinone imine through hydrolysis-oxidation. FeOx significantly adsorbs organic matter, calcium, and phosphate, which in turn influences OMP removal. Organic matter on field sand surfaces limits OMP removal by blocking sorption sites on the oxides. However, calcium and phosphate on field sand support benzotriazole removal via surface complexation and hydrogen bonding. This paper provides further insight into the abiotic removal mechanisms of OMPs in field RSFs.

1. Introduction

The presence of organic micropollutants (OMPs) in groundwater has become a challenge for drinking water production due to the potential risks they pose to public health (Gaston et al., 2019; Osenbrück et al., 2007). One economical way to remove OMPs from drinking water is to use existing treatment facilities at drinking water production plants (DWPPs). Certain process steps contribute to OMP removal at DWPPs, including activated carbon filtration (Piai et al., 2019), membrane filtration (Khanzada et al., 2020; Osorio et al., 2022), and advanced oxidation (Benner and Ternes, 2009; Yang et al., 2017). However, these processes involve substantial investment and maintenance costs, and are rarely used to treat groundwater. Thus, more investigation is needed to explore OMP removal in existing cost-effective treatment processes for groundwater purification.

Rapid sand filters (RSFs) are regarded as inexpensive and sustainable, and they have the potential to remove OMPs from groundwater (Benner et al., 2013; Wang et al., 2021b). RSFs in groundwater treatment are typically designed to remove ammonia (Lee et al., 2014), residual methane (Poghosyan et al., 2020), and reduced metal species (e.g., Fe(II), Mn(II), and As (III)) (Vries et al., 2017; Gude et al., 2016). RSFs also display ancillary benefits, contributing to removing different OMPs, including pharmaceuticals (Zuehlke et al., 2007; Zearley and Summers, 2012), pesticides (Albers et al., 2015), and natural toxins (Ho et al., 2006; Mrkajic et al., 2021). Most previous studies focus on the biological removal processes of OMPs in RSFs (Hedegaard and Albrechtsen, 2014; Papadopoulou et al., 2019). Yet, abiotic removal processes and mechanisms of OMPs have not been well investigated in these systems.

Iron oxides (FeOx) and manganese oxides (MnOx) in sand coating layers have significant potential to remove OMPs through abiotic processes. An important function of RSFs is oxidation of Fe(II) and Mn(II).

* Corresponding author.
E-mail address: nora.sutton@wur.nl (N.B. Sutton).
[1] Present address: Division of Soil and Water Management, Faculty of Bioscience Engineering, KU Leuven, Belgium.
[2] Present address: Infrastructure and Environment, School of Engineering, University of Glasgow, Glasgow, UK.
[3] Present address: Nijhuis Saur Industries, Doetinchem, the Netherlands.

https://doi.org/10.1016/j.watres.2023.120146
Received 28 December 2022; Received in revised form 29 April 2023; Accepted 28 May 2023
Available online 30 May 2023

Regular backwashing is used to remove FeOx and MnOx to prevent clogging, but residual oxides can still remain on sand granules, resulting in FeOx/MnOx-coated sand (Hedegaard et al., 2014). Adsorption and oxidation are two potential pathways involved in OMP removal by FeOx/MnOx (Feitosa-Felizzola et al., 2009; Huguet et al., 2013). FeOx reportedly enhances the adsorption of clarithromycin and roxithromycin (Feitosa-Felizzola et al., 2009), while MnOx improves the removal of microcystin-LR (Kumar et al., 2020). However, few studies show the performance of field formed FeOx/MnOx on OMP removal. In addition, knowledge about underlying mechanisms of adsorption and oxidative transformation of OMPs with FeOx and MnOx are scarce, especially for those oxides formed in field RSFs.

Compared to synthetic pure oxides or mineral ore, FeOx and MnOx formed in field RSF may have different performances for OMP removal due to the different coating compositions on sand surfaces. During field filtration processes, other components may be incorporated in the amorphous or crystalline FeOx/MnOx structures. FeOx/MnOx-coated sand surfaces can adsorb other contaminants (e.g., organic matter, phosphate, and (heavy) metals) (Ding and Shang, 2010; Lai and Chen, 2001; Singh et al., 1984) or be covered with biofilm (Bar-Zeev et al., 2012). These contaminants may block adsorption sites or change the adsorption capacities of field FeOx and MnOx for OMP removal. Accordingly, it is important to explore the performance of field FeOx/MnOx-coated sand on OMP removal and to understand the effect of the coating composition on OMP removal.

This study investigates OMP removal by FeOx and MnOx coated sand in field RSFs. Field FeOx/MnOx-coated sand from two RSFs – including primary RSF and secondary RSF – were applied to assess their capacities for OMP removal. The field collected sand were characterized in order to determine the surface coating compositions. In addition, FeOx and MnOx were separately coated on clean sand surfaces as synthetic FeOx- and MnOx-coated sand, which were used to assess the individual contributions of FeOx and MnOx to OMP removal. Additionally, we explored the effects of other coating components (i.e., organic matter, phosphate, and calcium) on OMP removal by separately adsorbing them onto synthetic FeOx-coated sand. Adsorption isotherms coupled with the sand surface characterization provide insights into the OMP adsorption mechanisms. TPs were measured to unravel the oxidative transformation pathways of OMPs. This study offers a deeper understanding of the abiotic removal processes and mechanisms of OMPs in field RSFs.

2. Materials and methods

2.1. Sand material

Field sand material was collected from two groundwater-fed RSFs operated in series by Evides Water Company (Rotterdam, the Netherlands), namely Primary-RSF sand (Pri_sand) and Secondary-RSF sand (Sec_sand) (see details in Text S1). The preparation methods of synthetic FeOx-coated sand (FeOx_sand) and synthetic MnOx-coated sand (MnOx_sand) were derived from previous investigations (Stenkamp and Benjamin, 1994; Bajpai and Chaudhuri, 1999) (see Text S2). Three negative control batches were also set with clean sand, clean Pri_sand, and clean Sec_sand. Clean sand materials were washed three times in nitrohydrochloric acid and three times in MilliQ water to remove the oxide coating layer. Negligible concentrations of Fe and Mn on clean sand materials indicated washing was sufficient (Fig. S1a).

2.2. Chemicals and reagents

Five pesticides (2,6-dichlorobenzamide (BAM), mecoprop, 2,4-dichlorophenoxyacetic acid (2,4-D), chloridazon, and bentazone), five pharmaceuticals (paracetamol, salicylic acid, caffeine, iomeprol, and ioxitalamic acid), and one industrial chemical (benzotriazole) were selected as model compounds (listed in Table S1). These compounds have been detected in European drinking water sources and are considered priority OMPs for drinking water production (Hedegaard et al., 2014; Sjerps et al., 2019). OMP purchase and stock information is given in Text S3.

2.3. Characterization of sand materials

Sand surfaces were characterized prior to the batch experiments. FeOx, MnOx, and other components coated on each sand material were dissolved through microwave digestion (See details in Text S4). The concentrations of Fe, Mn, and multiple elements (see Table S2) in (diluted) samples were measured for the quantification of FeOx, MnOx, (heavy) metals, and nonmetals on the sand surface, respectively. Organic matter on sand surfaces were quantified by measuring the concentration of total organic carbon (TOC) with an elemental analyzer (CHN EA1108, Carlo Erba, Italy). X-ray diffraction (XRD) (D8 advance, Bruker, USA) was used to analyze the crystalline species on sand surfaces. X-ray photoelectron spectroscopy (XPS) (Axis Ultra, Kratos Analytical, UK) was conducted to reveal the chemical states of Fe/Mn and the C/N species. The chemical bonds and functional groups on sand surfaces were analyzed by using the Attenuated total reflectance - Fourier transform infrared spectroscopy (ATR-FTIR) (ALPHA II, Bruker, USA). The sand surface charge was determined by measuring the point-of-zero charge (pH_{pzc}) through a modified salt titration method (Tan et al., 2008). Text S5 contains further information of above analysis.

2.4. Adsorption experiment

To perform kinetic and equilibrium adsorption studies, material was added in serum bottles containing a mixture of 11 OMPs and tap water with 20 mM NaN_3, to inhibit microbial activity. Bottles were shaken horizontally at 120 rpm at 20 °C and wrapped in aluminum foil to avoid OMP photodegradation. Samples were collected from each bottle with a volume of 0.8 mL, then centrifuged at 15,000 rpm for 10 min. The supernatant was diluted, if needed, and stored at −20 °C until analysis. Each bottle was operated and analyzed in duplicate.

The amount of adsorbed OMPs and their normalized concentration (C/C_0) and removal percentages were calculated as follows:

$$q_t = \frac{C_0 - C_t}{m} \times V \quad (1)$$

$$q_e = \frac{C_0 - C_e}{m} \times V \quad (2)$$

$$Rp = \frac{C_0 - C_t}{C_0} \times 100 \quad (3)$$

where q_t (μg/g) is the mass of OMP removed by per gram of sand at the sampling time t; q_e (μg/g) represents the removed amount of OMP at equilibrium; C_0 (μg/L) is initial concentration of OMP; C_t (μg/L) is OMP concentration at sampling time; C_e (μg/L) is OMP concentration at adsorption equilibrium; m (g) is sand mass added; V (L) is liquid volume; Rp (%) is the removal percentage of OMP.

2.4.1. Kinetic experiment

A kinetic experiment was performed with 20 g sand and 100 mL liquid with the initial OMP concentration of 1 mg/L (Fig. S2). Four prepared sand materials, including Pri_sand, Sec_sand, FeOx_sand, and MnOx_sand, were applied. Samples were collected at 0 min, 5, 15, and 30 min, then 1, 3, 6, 12, 24, 48, 80, and 168 h. In negative control batches, samples were only collected at 0 min and 168 h. The total removal efficiencies of OMPs were calculated with the concentrations of OMPs at 0 min and 168 h. The samples collected at 168 h were used for TP analysis. Another kinetic experiment was conducted with a trace OMP concentration of 1 μg/L. The samples were taken at 30 min, 1, 4, 20, 48, and 74 h. Iomeprol and ioxitalamic acid were not included in this study, as analytical methods were not available at trace concentrations.

Total sampled volume was less than 9% of the initial solution volume.

2.4.2. Isotherm experiment

In the isotherm experiment, seven different initial concentrations of OMP were used: 0.5, 0.7, 1, 3, 5, 7, and 10 mg/L (Fig. S2). Four different types of sand, including FeOx_sand, MnOx_sand, Pri_sand, and Sec_sand, were used in different batches. Sand mass and liquid volume were 10 g and 50 mL, respectively. The kinetic experiments showed that adsorption reached equilibrium condition by 80 h at the latest (Figs. S3 and S4). Therefore, equilibrium concentrations were measured at 80 h. The Freundlich model (Eq. (4)) was used to fit experimental data and evaluate the adsorption equilibrium state with different sand materials.

$$q_e = K_F C_e^n \quad (4)$$

where q_e (μg/g) represents the adsorbed amounts of OMP at equilibrium; C_e (μg/L) is OMP concentration at adsorption equilibrium; K_F ($\mu g^{1-n} \bullet g^{-1} \bullet L^n$) and n (dimensionless) are the constants of Freundlich models. The adsorbed amounts of OMPs at a fixed equilibrium concentration, as opposed to K_F values, were used to compare the affinities of studied sand materials with multiple OMPs. K_F values of Freundlich isotherm with a traditional unit ($\mu g^{1-n} \bullet g^{-1} \bullet L^n$) can cause serious anomalies during the assessment of relative adsorption capacity, as it also depends on the values of n (Bowman, 1982).

Accordingly, one value of C_e was chosen and substituted into Eq. (4) to determine $q_{e\gamma}$, where $\gamma = C_e$. The $q_{e\gamma}$ value for each OMP was used to compare the adsorption capacity of each sand for different OMPs. Fixed C_e was selected within the range of the isotherm data or to extrapolate the isotherm if needed. C_e was therefore defined as 3000 μg/L to compare the OMP adsorption capacities of different sand, and it was set as 500 μg/L to assess the differences between synthetic and field FeOx/MnOx, mainly depending on equilibrium concentration ranges. The values of q_{e3000} and q_{e500} values are given in Tables 1 and S3, respectively.

2.4.3. Coating matrix experiment

Coating matrix experiments were conducted to determine the effects of other coating substrates on OMP removal by field collected RSF sand. Based on the results of sand surface characterization, field sand was coated with high concentrations of OM, calcium, and phosphate (Fig. 2d). Dissolved organic matter (~ 500 mg C/L) (extracted from compost soil; method described in Wang et al., 2022a), $CaCl_2$ (~ 2 g Ca/L) and KH_2PO_4 (~ 0.8 g P/L) were added separately to 50 mL milliQ water in the bottles with synthetic FeOx_sand or MnOx_sand (10 g). The negative control was set as synthetic FeOx_sand or MnOx_sand with milliQ water. The initial and final concentrations of organic matter, total calcium, and total phosphate were quantified at 0 h and 48 h. Consequently, the liquid phase was replaced with tap water, then OMPs (1 mg/L each) and NaN_3 (20 mM) were spiked in the bottles. OMP concentrations were measured at 0 h and 80 h. Each bottle was operated and analyzed in triplicate.

2.5. Analytical methods

Concentrations of Fe, Mn, (heavy) metals and nonmetals (listed in Table S2) in aqueous samples were measured using inductively coupled plasma-optical emission spectrometry (ICP-OES) (Avio 500, PerkinElmer, USA). TOC concentrations in liquid samples were measured using a Shimadzu TOC-LCPH with an autosampler (Shimadzu ASI-L) (Text S5). OMPs at high concentrations(1 mg/L) were quantified using an ultra-performance liquid chromatography coupled with a diode array detector (UPLC-DAD) (Dionex ultimate 3000, Thermo Fisher Scientific, USA), connecting a CSH Phenyl-Hexyl column (1.7 μm, 2.1 × 150 mm) (Waters, USA), according to the method described in Wang et al. (2022b). The quantification of trace OMPs below 1 μg/L was performed on an Ultra High Performance Liquid Chromatography (UHPLC) equipped with a triple quad mass spectrometer (SCIEX Triple Quad™ 5500, USA) (see details in Wang et al. 2022a). TPs were analyzed using Ultimate 3000 high liquid chromatography coupled with a high-resolution accurate-mass spectrometer (LC-HRAM-MS) (Thermo Scientific, San Jose, USA) under a full-scan mode. Raw data obtained from duplicate measurements were processed using the software "Compound Discover" (version 3.3) (Thermo Scientific, USA). Text S6 describes the TPs' analytical method and date processing workflow. Multiple blank and control samples were also prepared to make the results more reliable. These are listed in Table S4.

2.6. Statistical analysis

The student's test (t-test) was applied to check the significance of each paired group for OMP removal. The statistical results were shown in figures, where "*" means p-value is 0.01 – 0.05; "**" means p-value is 0.001 – 0.01; "***" means p-value is 0.0001 – 0.001. Statistical analyses were performed using R (version 4.1.0).

3. Results and discussion

3.1. The performance of field FeOx/MnOx-coated sand on OMP removal

The full-scale RSFs normally consist of two filtration units for groundwater treatment. Sand collected from the primary RSF unit (Pri_sand) and the secondary RSF unit (Sec_sand) at a Dutch DWPP were used to assess the capacity of field FeOx/MnOx for OMP removal. Pri_sand removed paracetamol, salicylic acid, and benzotriazole (Fig. 1a), while Sec_sand only removed paracetamol (Fig. 1b). For comparison, the removal of OMPs with the clean field sand where the coating had been removed was very low in the range of 1.3% to 14.2%. (Fig. 1). Hence, we conclude that the removal of paracetamol, salicylic acid, and benzotriazole is due to the coating layers on the field sand particles. To understand the removal mechanisms of OMPs by field FeOx/MnOx-coated sand, we first characterized the coating compositions on the Pri_sand

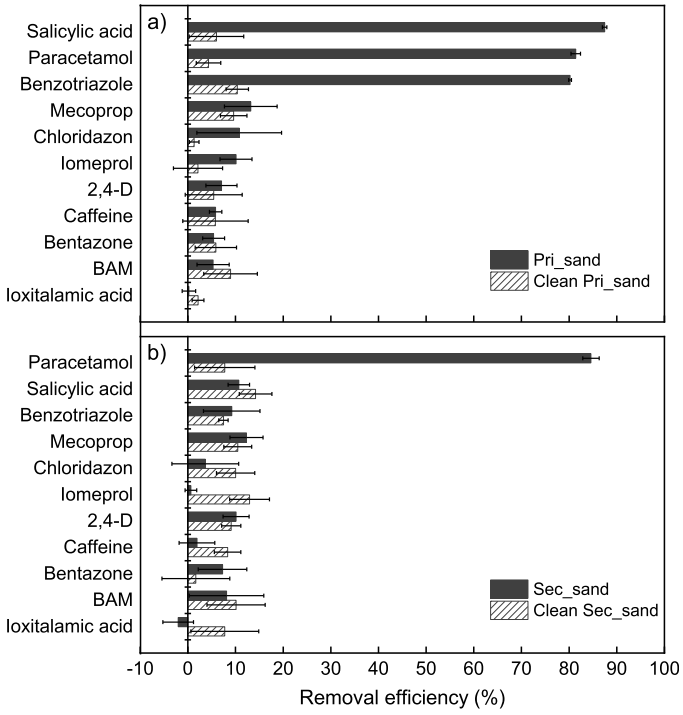

Fig. 1. Total removal efficiency of OMPs by (a) field primary-RSF sand (Pri_sand) and clean Pri_sand; (b) field secondary-RSF sand (Sec_sand) and clean Sec_sand. All the clean sands were used as reference materials (negative control).

and Sec_sand surfaces by measuring the amounts and valences of FeOx and MnOx as well as the concentrations of other components.

3.2. The surface characterization of field FeOx/MnOx-coated sand

The coating layers of two types of field sand (i.e., Pri_sand and Sec_sand) were characterized for (i) the concentrations of FeOx and MnOx, (ii) the valences of FeOx and MnOx, and (iii) the presence of other components such as organic matter, phosphate, and calcium. FeOx and MnOx co-existed on field collected sand, where the amount of FeOx was higher than MnOx, particularly on Pri_sand (Fig. 2a). This is due to (i) the concentration of Fe (10 mg/L) in the intake water being 50 times higher than that of Mn (0.2 mg/L), and (ii) the faster oxidation of Fe than that of Mn. As Fe could be largely removed in the primary RSF, more FeOx accumulated on Pri_sand (278.63 mg Fe·g^{-1}) (Fig. 2a). From XPS analysis, we could derive the valences of Fe and Mn on field-collected sand (Fig. 2b and 2c). The Fe $2p_{3/2}$ and Fe $2p_{1/2}$ peaks located around 711 eV and 724.6 eV suggested Fe (III) species were present on field collected sand (Fig. 2b) (Yamashita and Hayes, 2008). The Mn $2p_{3/2}$ peaks indicated Mn (III) and Mn (IV) co-existed on field RSF sand (Fig. 2c) (Ilton et al., 2016). The multiple valence states of Mn species are an important factor in Mn catalytic oxidation processes in field RSFs (Yang et al., 2020). There was no characteristic peak of crystalline FeOx and MnOx in XRD spectrum in any of the sand materials (Fig. S5), suggesting the oxide species were amorphous or poorly crystalline, as previously described by Liu et al. (2020) and Yang et al. (2020). Beside FeOx and MnOx, field sand was coated with large amounts of organic matter, phosphate, and calcium (Fig. 2d). As the primary RSF could largely remove these contaminants from intake water, Sec_sand was less coated with organic matter, phosphate, and calcium (Fig. 2d). This study therefore shows that there was a blend of FeOx and MnOx, as well as organic matter, phosphate, and calcium on the field RSF sand, especially in the primary RSF.

3.3. The removal mechanisms of OMPs by FeOx and MnOx

In order to further understand the removal mechanisms of OMPs by field FeOx/MnOx-coated sand, we focus on the individual roles of FeOx, MnOx, as well as the other coating components, i.e., organic matter, phosphate, and calcium. To this end, we measured the adsorption isotherms of OMPs onto synthetic FeOx-coated sand (FeOx_sand) and synthetic MnOx-coated sand (MnOx_sand) (Fig. 3). The XPS analysis showed that the valences of Fe and Mn on synthetic and field-collected sand were the same (Fig. S1b and S1c). In addition, we unraveled the effects of organic matter, phosphate, and calcium on OMP adsorption. Finally, TPs were analyzed to reveal the oxidative transformation pathways of OMPs with FeOx/MnOx-coated sand.

3.3.1. Chemical bonds between OMPs and FeOx

The presence of synthetic FeOx on sand surfaces enhanced OMP removal. The removal of all OMPs by clean sand was less than 10%, while FeOx_sand resulted in the removal of caffeine (100.0%), salicylic acid (93.2%), 2,4-D (89.8%), mecoprop (72.2%), paracetamol (71.4%), and iomeprol (31.6%) (Fig. S7). A proposed primary mechanism for

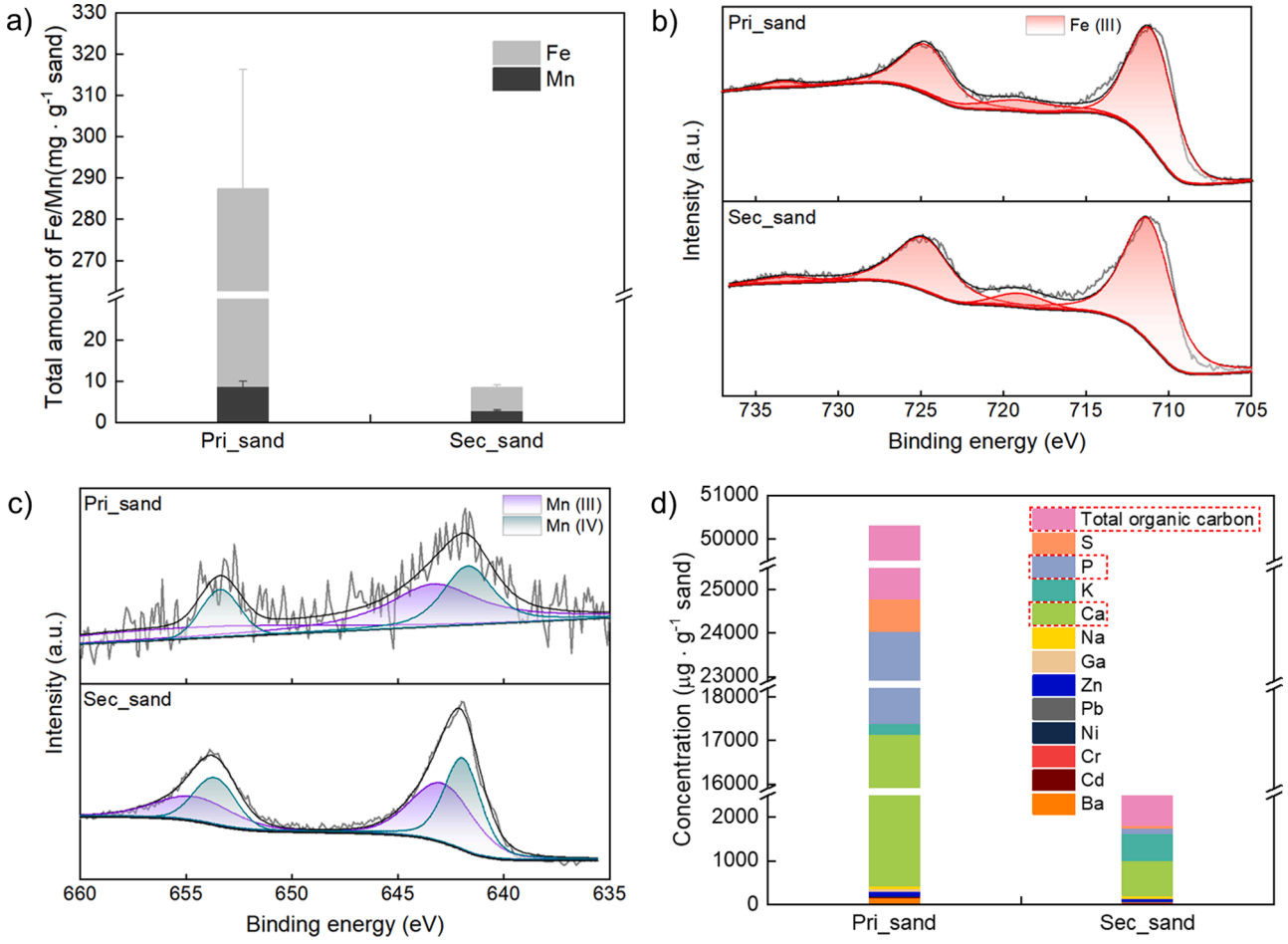

Fig. 2. The surface characterization of Primary-RSF sand (Pri_sand) and Secondary-RSF sand (Sec_sand). (a) The coating amounts of Fe and Mn oxides; (b) XPS spectrum of Fe 2p; (c) XPS spectrum of Mn 2p; (d) the coating amounts of organic matter and multiple elements. Organic matter was quantified by the total organic carbon (TOC), while the XPS spectrums of organic carbon and nitrogen were presented in Fig. S6.

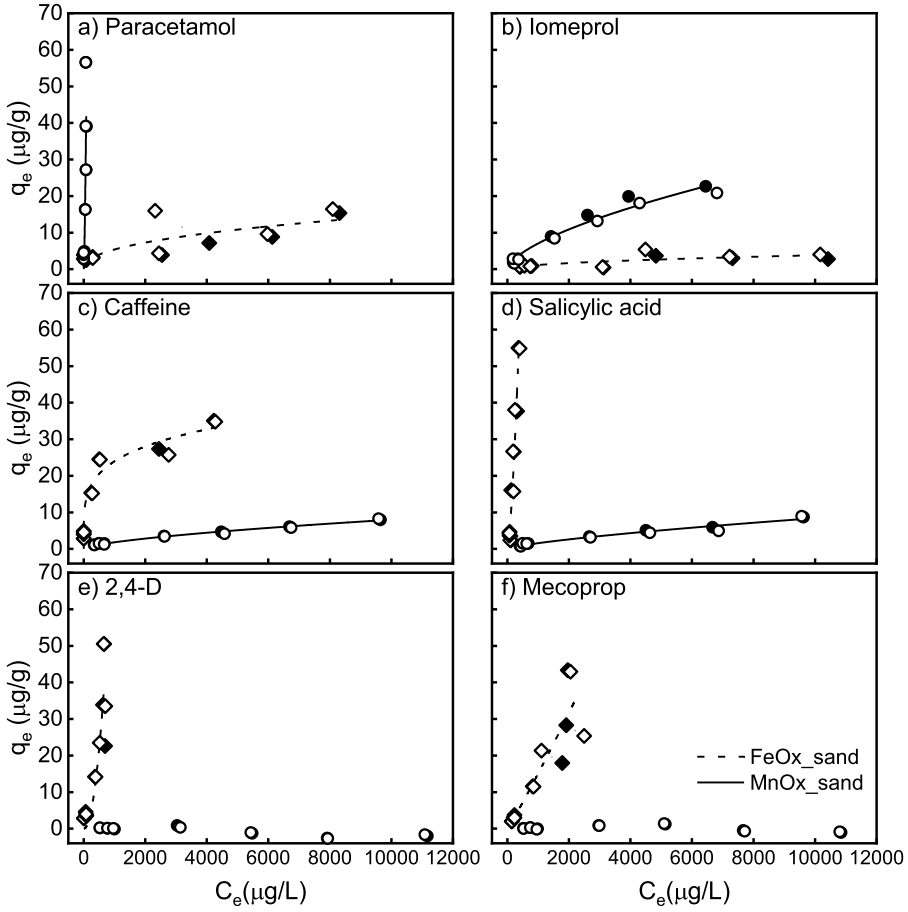

Fig. 3. Freundlich isotherm models for six OMPs removal by synthetic FeOx-coated sand (FeOx_sand) (diamond symbols) and synthetic MnOx-coated sand (MnOx_sand) (circle symbols). There is no fitting curve for 2,4-D and mecoprop removal by MnOx_sand due to their negligible removal. Hollow and solid symbols represent the duplicate bathes.

organic contaminants adsorption on mineral oxide surfaces is ligand exchange between mineral oxides and carboxyl and/or hydroxyl groups in organic compounds (Vindedahl et al., 2016). All the adsorbed OMPs (except for caffeine) contain carboxyl and/or hydroxyl groups, while the poorly removed compounds (excluding ioxitalamic acid) lack these two functional groups (Table S1), indicating that these groups are important for OMP adsorption onto FeOx.

FTIR spectroscopy was applied to identify the functional groups on FeOx after OMP adsorption. Compared with raw FeOx_sand (before adsorption), there were two characteristic bands at 1340.74 cm^{-1} and 2071.17 cm^{-1} (Fig. 4), which were assigned to the carboxylic group (Yost et al., 1990; Blber and Stumm, 1994) and azide (N=N=N) group that originate from NaN_3 (the biocide used in this study) (Eigler et al., 2013), respectively. The common valleys at 1600 cm^{-1} and 3300 cm^{-1} (Fig. 4) were due to spectral subtractions of interfacial H_2O and OH groups, respectively (Blber and Stumm, 1994; Tejedor-Tejedor et al., 1990). The bond to phenolic OH group was reportedly located at around 1260 cm^{-1} (Yost et al., 1990; Biber and Stumm, 1994), yet was not detected in spectrum. This is most likely due to the fact that the O-H bond in the phenolic group was weaker than the bond to the carboxylic group on FeOx (Blber and Stumm, 1994). Freundlich isotherm analysis showed FeOx had higher adsorption capacity for salicylic acid, 2,4-D, and mecoprop (the OMPs containing the carboxyl group) than other compounds (Fig. 3), as the values of q_{e3000} followed the order: salicylic acid > 2,4-*D* > mecoprop > caffeine > paracetamol > iomeprol (Table 1). These results indicate that the carboxyl group has greater affinity for FeOx than other functional groups, and plays an important role in OMP adsorption to FeOx. We therefore conclude that Pri_sand removes salicylic acid through bonding of carboxyl group with FeOx.

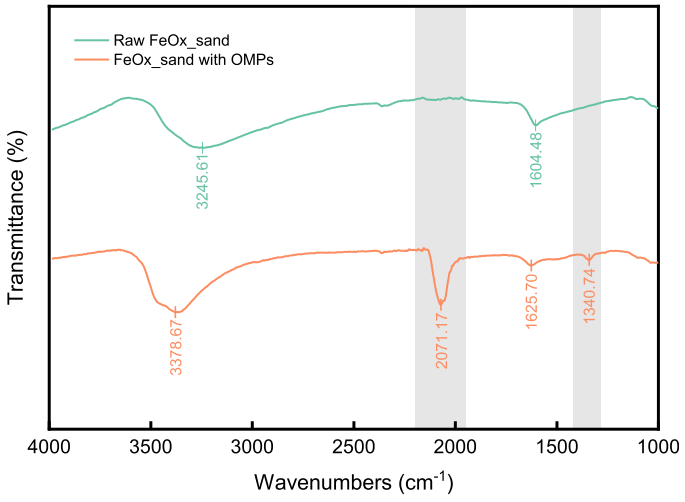

Fig. 4. FTIR spectra of raw synthetic FeOx-coated sand (FeOx_sand) (before OMP adsorption) and FeOx_sand with OMPs (after OMP adsorption).

To understand whether FeOx can further oxidize salicylic acid, we scanned TPs by using LC-MS/MS analysis in both positive and negative ion modes (Text S6). No known TPs of salicylic acid were observed in the samples treated by FeOx, suggesting that oxidation most likely did not occur. This was further confirmed in the kinetic experiment at trace

Table 1
Isotherm parameters for OMP removal by synthetic FeOx-coated sand (FeOx_sand), synthetic MnOx-coated sand (MnOx_sand), field primary-RSF sand (Pri_sand) and field secondary-RSF sand (Sec_sand).

Types of sand	OMPs	Freundlich isotherm parameters			
		K_F ($\mu g^{1-n} \bullet g^{-1} \bullet L^n$)	n	q_{e3000} [a] (μg/g sand)	R^2
FeOx_sand	Salicylic acid	7.82×10^{-3}	1.50	1262.62 [b]	0.97
	2,4-D	6.72×10^{-5}	2.04	842.21 [b]	0.81
	Mecoprop	9.33×10^{-3}	1.07	48.82 [b]	0.82
	Caffeine	5.08	0.22	30.67	0.90
	Paracetamol	0.27	0.43	8.67	0.64
	Iomeprol	0.03	0.52	2.04	0.51
MnOx_sand	Paracetamol	0.05	1.52	10,350.04 [b]	0.71
	Iomeprol	0.09	0.63	14.03	0.98
	Caffeine	0.02	0.65	3.67	0.99
	Salicylic acid	0.01	0.73	3.50	0.96
Pri_sand	Paracetamol	1.08×10^{-3}	1.64	550.52 [b]	0.83
	Salicylic acid	0.02	1.02	85.59 [b]	0.98
	Benzotriazole	0.03	0.87	33.51	0.99
Sec_sand	Paracetamol	0.03	1.12	257.09 [b]	0.89

[a] the value of γ (C_e) is defined as 3000 μg/L;.
[b] the largest equilibrium concentrations of OMPs are even lower than 3000 μg/L, for comparison with other OMPs, the isotherms need to be extrapolated.

concentrations of 1 μg/L (for each compound). Salicylic acid was significantly removed by FeOx_sand (Fig. 5a), but was released from field Pri_sand and Sec_sand, resulting in equilibrium concentrations of 7.9 ± 0.4 μg/L and 18.7 ± 0.7 μg/L, respectively (Fig. 5b). As salicylic acid showed the greatest affinity to FeOx (Table 1), the released salicylic acid most likely originated from the accumulative adsorption of salicylic acid onto field formed FeOx. The desorption of salicylic acid indicated that salicylic acid is most likely not oxidized by FeOx.

3.3.2. Electrostatic adsorption and oxidation of OMPs by MnOx

MnOx_sand enhanced the removal of four pharmaceuticals, including paracetamol (94.3%), iomeprol (79.7%), salicylic acid (31.1%), and caffeine (26.1%) (Fig. S7). It has been shown previously that adsorption was the first step for OMP removal by MnOx (Forrez et al., 2009; Zhang and Huang, 2005), whereby electrostatic interactions played an important role. The pH point of zero charge (pH_{pzc}) of MnOx_sand is 5.08 (Fig. S8), suggesting the surface of MnOx is negatively charged at neutral pH. Both 2.4-D (pKa = 2.81) and mecoprop (pKa = 3.47) are negatively charged at neutral pH and hence an electrostatic repulsive force existed between the 2,4-D and mecoprop anions and MnOx surface, resulting in negligible removal (Fig. 3e and 3f). The removal capacity of MnOx for the four adsorbed pharmaceuticals was different, as values of q_{e3000} was (in order): paracetamol >> iomeprol > caffeine ≈ salicylic acid (Table 1). Both paracetamol (pKa = 9.46) and iomeprol (pKa = 11.73) were protonated at neutral pH. The electrostatic attractive force between these protonated molecules and MnOx promoted their adsorption. As a neutral compound with neither carboxyl nor hydroxyl groups (Liu et al., 2022), caffeine shows a lower adsorption affinity to MnOx (Fig. 3c). Overall, electrostatic interactions dominate the adsorption process. The protonated OMPs with positive charge were adsorbed more effectively to MnOx than neutral or negatively charged molecules.

Following adsorption, MnOx is able to oxidatively degrade certain OMPs. Mn^{2+} concentration increased in the aqueous solution during the kinetic experiments (Fig. S9), suggesting OMP oxidation occurred. According to LC-MS/MS analysis in both positive and negative ion modes, the peak corresponding to an oxidative by-product of paracetamol described by Zhong et al. (2019) was also detected in our samples treated with MnOx_sand (Fig. 6a), Pri_sand (Fig. 6b), and Sec_sand (Fig. 6c). The peaks at m/z of 150.05 and 106.03 correspond with paracetamol and *p*-benzoquinone imine structures, respectively (Fig. 6a). The peak of *p*-benzoquinone imine was not present in control samples (Fig. 6a, 6b, and 6c), which is additional evidence for paracetamol oxidation by MnOx. The quinone-imine structure likely originated from the hydrolysis of the amido group in paracetamol and further oxidation of the aminophenol ring (Fig. 6d). Hydrolysis-oxidation was proposed as a main degradation pathway for the phenolic compounds treated by MnOx (Stone and Morgan, 1984; Zhong et al., 2019). Overall, MnOx present on Pri_sand and Sec_sand contributed to paracetamol removal through adsorption and oxidation.

3.4. The effects of organic matter on OMP adsorption

Field FeOx/MnOx-coated sand showed less capacity for OMP adsorption than synthetic FeOx/MnOx-coated sand. Four OMPs, namely 2,4-D, mecoprop, caffeine, and iomeprol, were adsorbed to synthetic oxides (Fig. 3), but were not removed by field FeOx/MnOx coated sand (Fig. 1). On the other hand, field sand did remove salicylic acid and paracetamol (Fig. 1). To compare the capacities of field and synthetic oxides on OMP removal, the adsorbed amounts of salicylic acid and paracetamol at equilibrium were normalized on the coated amounts of FeOx and MnOx, respectively (Fig. 7). The q_{e500} values of salicylic acid were 4.15 μg/mg Fe for synthetic FeOx and 0.05 μg/mg Fe for field FeOx coated on Pri_sand (Table S3). For paracetamol, these were: 189.97 μg/mg Mn for synthetic MnOx, 3.35 μg/mg Mn for field MnOx coated on Pri_sand, and 11.86 μg/mg Mn for field MnOx coated on Sec_sand (Table S3). The lower capacity of field formed FeOx/MnOx for OMP adsorption is likely due to the adsorbed organic matter on field sand

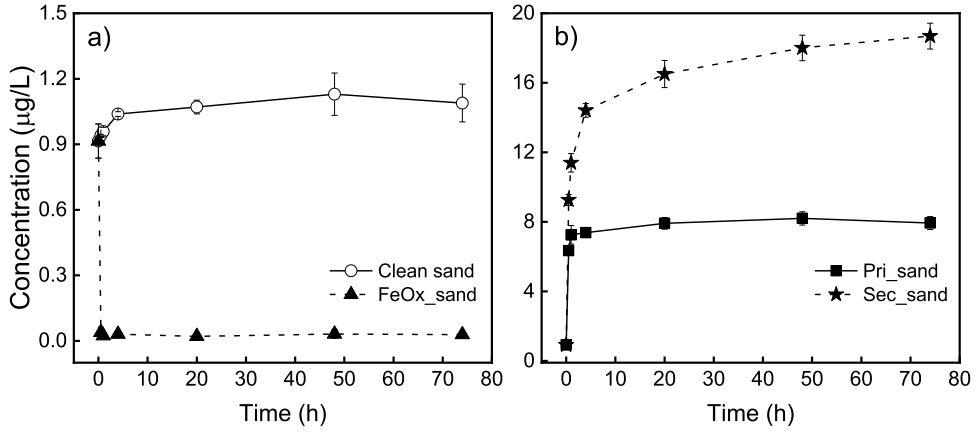

Fig. 5. The concentration of salicylic acid over time in the kinetic experiment at an initial concentration of approximately 1 μg/L. (a) The adsorption of salicylic acid to synthetic FeOx-coated sand (FeOx_sand); (b) the desorption of salicylic acid from field collected sand (primary-RSF sand (Pri_sand) and secondary-RSF sand (Sec_sand)).

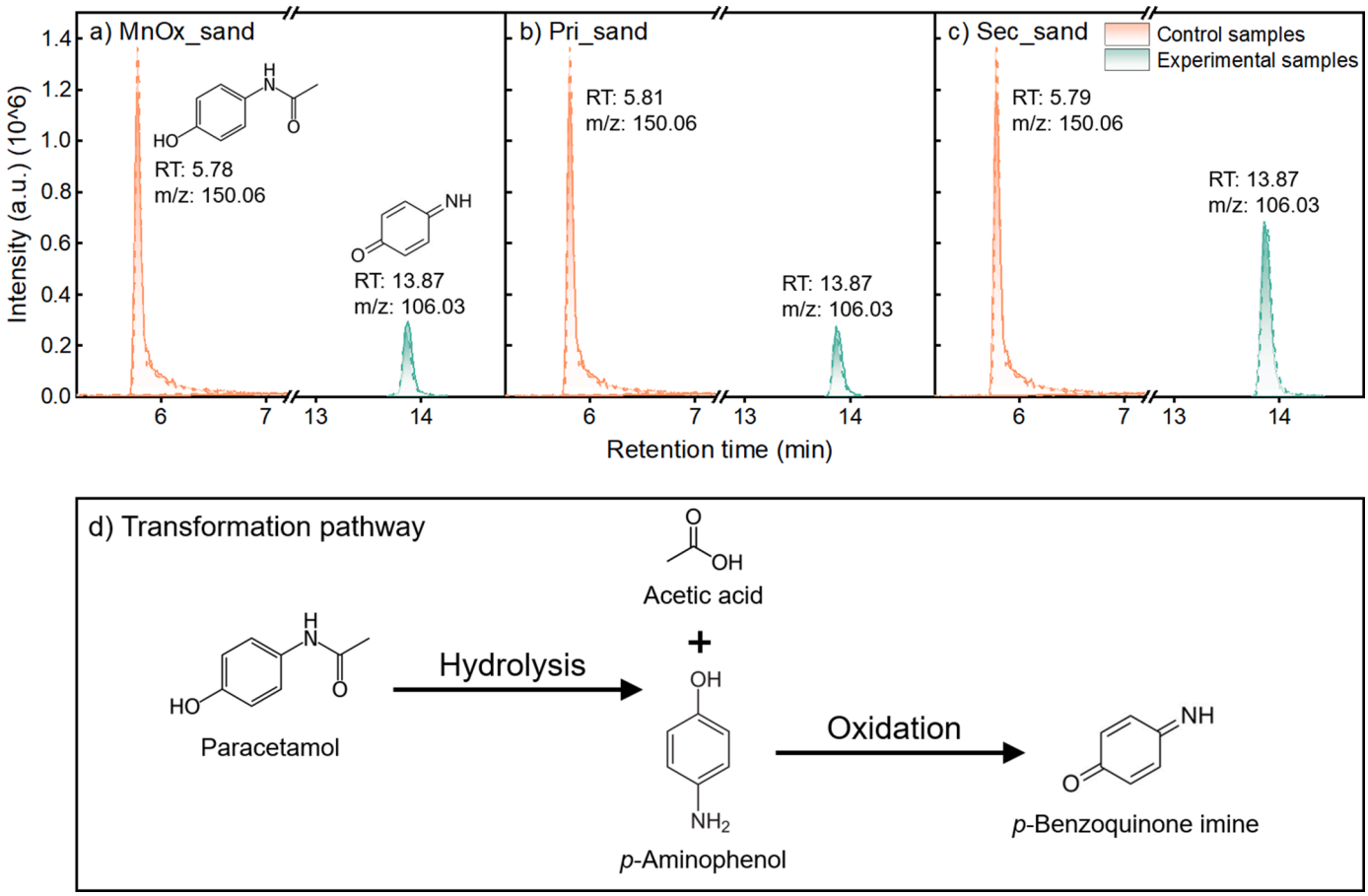

Fig. 6. Oxidative degradation of paracetamol by MnOx. (a) the chromatograms of control samples (treated with clean sand) and experimental samples (treated with synthetic MnOx-coated sand (MnOx_sand)); (b) the chromatograms of control samples (treated with clean sand) and experimental samples (treated with field primary-RSF sand (Pri_sand)); (c) the chromatograms of control samples (treated with clean sand) and experimental samples (treated with field secondary-RSF sand (Sec_sand)) (The solid and dot lines represent the duplicate analysis), all the individual chromatogram and *m/z* information were shown in Figure S10; d) the proposed transformation pathway of paracetamol.

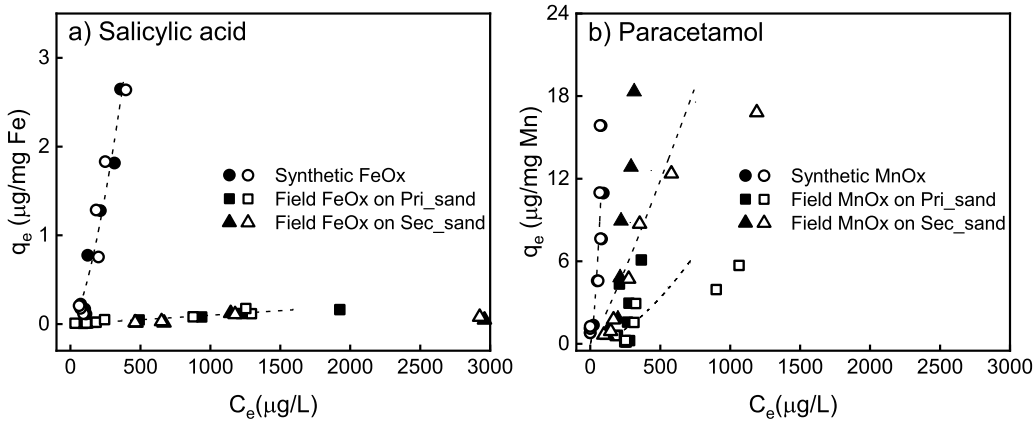

Fig. 7. The adsorption capacities of field and synthetic iron/manganese oxides (FeOx/MnOx) on OMP adsorption. (a) the adsorption isotherms of salicylic acid by field and synthetic FeOx (There is no fit line for the isotherm data of salicylic acid for field FeOx on Sec_sand due to the negligible removal); (b) the sorption isotherms of paracetamol by field and synthetic MnOx. Data fit the Freundlich isotherm model. Hollow and solid symbols represent the duplicate batches.

(Fig. 2d).

To confirm the effects of organic matter on OMP adsorption, we adsorbed compost organic matter on synthetic sand and then studied the removal of OMPs. FeOx_sand was able to remove 85.4% of compost organic matter (Fig. S11). The presence of organic matter on synthetic FeOx_sand significantly reduces the removal efficiencies of salicylic acid, caffeine, 2,4-D, and mecoprop (Fig. 8). The adsorbed organic matter competes for OMP adsorption sites on FeOx, as carboxyl and/or hydroxyl groups present in organic matter could strongly bond on FeOx surface (Gu et al., 1994). The coating mass ratio of organic matter (mg $C \cdot g^{-1}$ sand) / FeOx (mg $Fe \cdot g^{-1}$ sand) on Sec_sand (0.23) was higher than that on Pri_sand (0.09). Therefore, more organic matter competed for

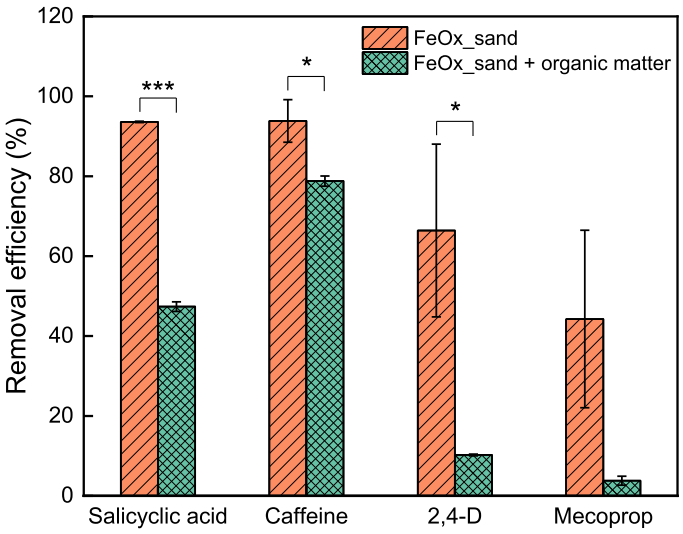

Fig. 8. The removal efficiency of OMPs by synthetic FeOx-coated sand (FeOx_sand) and the FeOx_sand with organic matter. Student's test (*t*-test) was used to check the significance of each paired group for OMP removal, "*" means p-value is 0.01–0.05; "**" means p-value is 0.001–0.01; "***" means p-value is 0.0001–0.001.

OMP adsorption sites on Sec_sand, resulting in a limited removal of salicylic acid by Sec_sand (Fig. 1b).

The removal of compost organic matter by MnOx_sand was negligible (Fig. S11), since fulvic acids and humic acids in compost organic matter are both negatively charged at neutral pH (Bob and Walker, 2001; Palomino and Stoll, 2013), and the electrostatic repulsive force suppressed adsorption of compost organic matter onto MnOx_sand. Interestingly, the adsorption isotherms showed that MnOx coated on Pri_sand had a lower capacity for paracetamol removal than that on Sec_sand (Fig. 7b). The coating mass ratio of organic matter (mg C·g^{-1} sand) / MnOx (mg Mn·g^{-1} sand) on Pri_sand (2.94) was rather higher than that on Sec_sand (0.44). Thus, we conclude that organic matter present on field sand can compete for active sites of MnOx for paracetamol removal, as also previously shown by Huguet et al. (2014). Overall, the organic matter present on field sand have occupied the adsorptive sites of FeOx and MnOx, hence limiting OMP adsorption.

Benzotriazole was neither removed by FeOx_sand nor MnOx_sand (Fig. S7), but showed a high affinity for Pri_sand (Fig. 9a). Thus, the other adsorbed components, except for FeOx and MnOx, might play important roles during benzotriazole adsorption. Compared with other sands, Pri_sand surface contains large amounts of organic matter, in addition to FeOx (Figs. 3d and S1d). However, the FeOx_sand with compost organic matter negligibly removed benzotriazole (Fig. 9b). The adsorption of benzotriazole to organic matter is mainly due to van der Waal forces, which is a weak bonding interaction (Rhodes-Dicker and Passesport, 2019; Yu et al., 2009). Thus, only limited amounts of benzotriazole were adsorbed to organic matter (Rhodes-Dicker and Passesport, 2019). In addition, the final adsorbed amount of organic matter on FeOx_sand (1671.9 μg C / g sand) was significantly lower than that on Pri_sand (25,517.6 μg C / g sand) (Fig. S12). Thus, there were fewer interaction sites of organic matter available for benzotriazole adsorption. The low affinity combined with limited adsorption sites resulted in a negligible removal of benzotriazole with organic matter on FeOx_sand (Fig. 9b). However, the organic matter species on field sand may differ from compost organic matter used here. Thus, it is worthwhile investigating the effects of different organic matter amounts and various organic matter species on benzotriazole adsorption.

3.5. The effects of phosphate and calcium on OMP adsorption

Beside organic matter, Pri_sand surface also contains large amounts of phosphate and calcium (Fig. 2d). To determine their roles in benzotriazole removal, we used FeOx_sand and MnOx_sand to separately adsorb phosphate and calcium. MnOx_sand showed limited adsorption capacity for phosphate and calcium (Fig. S11). The small amounts of phosphate and calcium adsorbed on MnOx_sand had little effect on OMP removal (Fig. S13). In contrast, FeOx_sand more significantly adsorbed phosphate and calcium (Fig. S11), although the adsorbed amounts of phosphate and calcium on FeOx_sand were still lower than that of Pri_sand (Fig. S12), which was most likely due to the lower amounts of FeOx in the coatings on synthetic sand compared with Pri_sand (Fig. S1a). Therefore, FeOx_sand with phosphate or calcium were tested for benzotriazole adsorption.

In the presence of phosphate and calcium, the removal of benzotriazole by FeOx_sand increased from −4.5% to 92.2% and 62.9%, respectively (Fig. 9b). It has been shown that the co-existence of benzotriazole and Na_2HPO_4 reportedly enhanced corrosion protection on reinforcing steel, where FeOx adsorbed HPO_4^{2-}, then benzotriazole could adsorb on top of HPO_4^{2-} via hydrogen bonding (Wang et al., 2021a). Additionally, Bi et al. (2007) showed that an increase of Ca^{2+} density on a solid surface enhances the adsorption of benzotriazole to soil sediments due to surface complexation. Increasing Ca^{2+} concentration in

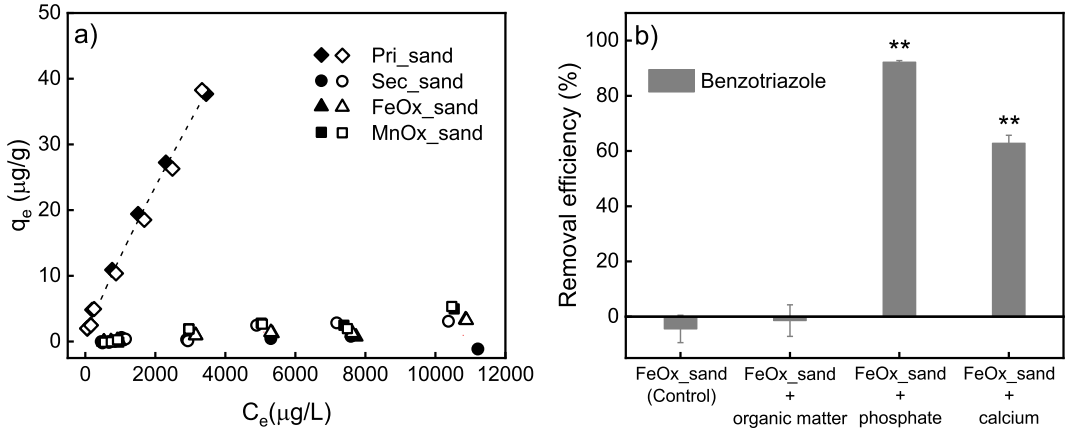

Fig. 9. Benzotriazole removal behaviors. (a) The adsorption isotherms of benzotriazole by synthetic FeOx-coated sand (FeOx_sand), synthetic MnOx-coated sand (MnOx_sand), field primary-RSF sand (Pri_sand) and field secondary-RSF sand (Sec_sand). There is no fitting curve for benzotriazole removal by FeOx_sand, MnOx_sand and Sec_sand due to its negligible removal. Hollow and solid symbols represent the duplicate bathes; (b) the removal efficiency of benzotriazole with the presence of organic matter, phosphate, and calcium on FeOx_sand. Student's test (*t*-test) was used to check the significance of each paired group for OMP removal, "*" means p-value is 0.01–0.05; "**" means p-value is 0.001–0.01; "***" means p-value is 0.0001–0.001.

aqueous solution also promotes benzotriazole adsorption, as the [benzotriazole + Ca^{2+}] complex can react with mineral surface sites of soil sediments (Bi et al., 2007; Wagner et al., 2020). This shows benzotriazole can interact with the adsorbed phosphate and/or calcium species on sand surfaces, forming [benzotriazole + HPO_4^{2-}] and/or [benzotriazole + Ca^{2+}] complexes, which explains the high removal of benzotriazole by field Pri_sand used for groundwater treatment.

3.6. Implications for RSFs used in the field

The proposed removal mechanisms for OMPs by FeOx and MnOx in RSFs are summarized in Fig. 10. FeOx and MnOx significantly contribute to OMP removal, especially for ionic compounds with carboxyl and/or hydroxyl groups, hence the addition of synthetic FeOx/MnOx-coated sand in RSFs can be a strategy to enhance OMP removal. However, in field conditions, adsorbed compounds (i.e., organic matter, (heavy) metals, and phosphate) onto sand may block reactive sites, hence reducing the adsorption/oxidation potential of FeOx/MnOx for OMPs. Alternatively, FeOx/MnOx-coated sand can be added in the secondary filter instead of the primary filter, considering that most contaminants most likely will have been removed in the primary filter. Another challenge for OMP removal by FeOx/MnOx in field RSF is the limited contact time, as the typical empty bed contact time of field RSF is a few minutes to one hour (Wang et al., 2021b). We acknowledge that the batch scale experiments used in this study do not match the field condition where OMPs are removed by FeOx/MnOx-coated sand in a continuous mode. However, the kinetic experiment performed at trace concentrations (1 μg/L) showed that, within 30 min, FeOx_sand removed 95.8% of salicylic acid, 85.7% of paracetamol, 82.7% of 2,4-D and 58.2% of mecoprop; MnOx removed 78.8% of caffeine and 42.4% of paracetamol (Fig. S14). This indicates that FeOx/MnOx_sand has the potentials for trace OMP elimination within short hydraulic contact times. Still, their longevity needs to be studied in a continuous filter system with a natural water matrix before field application.

MnOx can oxidize certain OMPs, like paracetamol, which results in the release of Mn^{2+}, which can potentially cause secondary contamination to the treated water. On the other hand, Mn-oxidizing bacteria can oxidize Mn^{2+} back to MnOx (Hu et al., 2020), and the remaining MnOx can also autocatalytically oxidize Mn^{2+} (Bruins et al., 2015). However, some oxidative TPs, like quinones (the TPs of paracetamol), are even more toxic than their parent compounds (Huguet et al., 2014). MnOx may also oxidize other OMPs present in groundwater, resulting in different TPs, not fully studied here. Thus, a comprehensive detection and control of oxidative TPs is required in the field for RSF treated water.

Finally, FeOx and MnOx co-exist on field RSF sand, hence the interactions between FeOx and MnOx in OMP removal processes need to be comprehensively investigated in the future. In summary, our results highlight the importance of FeOx and MnOx in OMP removal, but also show TPs may be formed that could contaminate drinking water. Obviously, the field application of FeOx/MnOx-based materials to achieve long-term enhancement for OMP removal requires further investigation.

4. Conclusions

The processes and mechanisms for OMP removal by FeOx and MnOx were studied to obtain insights into the abiotic removal of OMPs in RSFs.

The main conclusions are as follows:

- Field RSF sand can adsorb salicylic acid through bonding of carboxyl group with FeOx.
- MnOx present on field RSF sand contribute to paracetamol removal through electrostatic adsorption and oxidation. Paracetamol is transformed into *p*-benzoquinone imine through oxidative degradation.
- The organic matter on field RSF sand competes for adsorption sites, reducing the adsorption capacities of FeOx/MnOx for OMPs.
- Both phosphate and calcium present on field sand surfaces enhance the adsorption of benzotriazole.
- This study highlights the significance of FeOx and MnOx in the abiotic removal of OMPs in RSFs. The control of oxidative TPs and the field application of FeOx/MnOx-based materials need further study.

CRediT authorship contribution statement

Jinsong Wang: Conceptualization, Methodology, Investigation, Formal analysis, Data curation, Software, Writing – original draft, Project administration. **David de Ridder:** Resources, Formal analysis, Writing – review & editing, Supervision. **Nora B. Sutton:** Writing – review & editing, Supervision, Funding acquisition. **Baptiste A.J.**

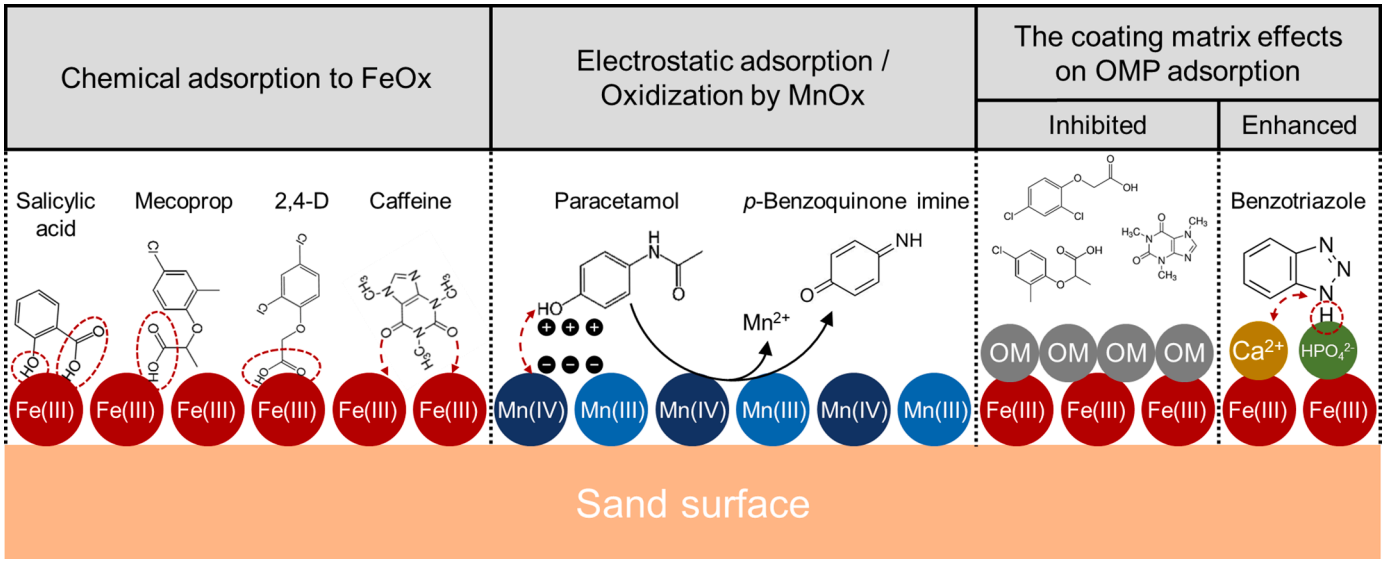

Fig. 10. The proposed schematic of OMP abiotic removal with FeOx/MnOx-coated sand in rapid sand filters (RSFs). The gray circle legend with "OM" represents "organic matter", the red circles label the functional groups for forming chemical bonding, the red arrows highlight the interactions between OMP molecules and coating species.

Poursat: Writing – review & editing, Supervision. **Pradip Saha:** Methodology, Software. **Albert van der Wal:** Conceptualization, Formal analysis, Writing – review & editing, Supervision, Funding acquisition.

Declaration of Competing Interest

The authors declare that they have no known competing financial interests or personal relationships that could have appeared to influence the work reported in this paper.

Data availability

Data will be made available on request.

Acknowledgments

The authors are sincerely thankful to Evides Water Company N.V. (Rotterdam, The Netherlands) and China Scholarship Council (CSC, File No. 201804910659) for financial support. We also would thank Ruili Yang (Chinese Academy of Sciences) and Barend van Lagen (Laboratory of Organic Chemistry, WUR) for helping with XPS analysis, Jie Li (National University of Singapore) for his help to adsorption data analysis, Chang Gao for her assistance with FTIR analysis, and Marko Pranic for his suggestions on pHpzc analysis. Finally, we acknowledged Pieter Gremmen, Livio Carlucci, and Marco Blokland (WFSR, WUR) for their assistance during ICP and LC analyses.

Supplementary materials

Supplementary material associated with this article can be found, in the online version, at doi:10.1016/j.watres.2023.120146.

References

Albers, C.N., Feld, L., Ellegaard-Jensen, L., Aamand, J., 2015. Degradation of trace concentrations of the persistent groundwater pollutant 2,6-dichlorobenzamide (BAM) in bioaugmented rapid sand filters. Water Res. 83, 61–70.
Bajpai, S., Chaudhuri, M., 1999. Removal of arsenic from ground water by manganese dioxide–coated sand. J. Environ. Eng. 125 (8), 782–784.
Bar-Zeev, E., Belkin, N., Liberman, B., Berman, T., Berman-Frank, I., 2012. Rapid sand filtration pretreatment for SWRO: microbial maturation dynamics and filtration efficiency of organic matter. Desalination 286, 120–130.
Benner, J., Helbling, D.E., Kohler, H.P.E., Wittebol, J., Kaiser, E., Prasse, C., Ternes, T.A., Albers, C.N., Aamand, J., Horemans, B., Springael, D., Walravens, E., Boon, N., 2013. Is biological treatment a viable alternative for micropollutant removal in drinking water treatment processes? Water Res. 47 (16), 5955–5976.
Benner, J., Ternes, T.A., 2009. Ozonation of metoprolol: elucidation of oxidation pathways and major oxidation products. Environ. Sci. Technol. 43 (14), 5472–5480.
Bi, E., Schmidt, T.C., Haderlein, S.B., 2007. Environmental factors influencing sorption of heterocyclic aromatic compounds to soil. Environ. Sci. Technol. 41 (9), 3172–3178.
Biber, M.V., Stumm, W., 1994. An *in-situ* ATR-FTIR study: the surface coordination of salicylic acid on aluminum and iron(III) oxides. Environ. Sci. Technol. 28 (5), 763–768.
Bob, M., Walker, H.W., 2001. Enhanced adsorption of natural organic matter on calcium carbonate particles through surface charge modification. Colloids Surf. A 191 (1–2), 17–25.
Bowman, B.T., 1982. Conversion of Freundlich adsorption K values to the mole fraction format and the use of SY values to express relative ddsorption of pesticides. Soil Sci. Soc. Am. J. 46, 740–743.
Bruins, J.H., Petrusevski, B., Slokar, Y.M., Huysman, K., Joris, K., Kruithof, J.C., Kennedy, M.D., 2015. Biological and physico-chemical formation of Birnessite during the ripening of manganese removal filters. Water Res. 69, 154–161.
Ding, C., Shang, C., 2010. Mechanisms controlling adsorption of natural organic matter on surfactant-modified iron oxide-coated sand. Water Res. 44, 3651–3658.
Eigler, S., Hu, Y., Ishii, Y., Hirsch, A., 2013. Controlled functionalization of graphene oxide with sodium azide. Nanoscale 5, 12136–12139.
Feitosa-Felizzola, J., Hanna, K., Chiron, S., 2009. Adsorption and transformation of selected human-used macrolide antibacterial agents with iron(III) and manganese (IV) oxides. Environ. Pollut. 157 (4), 1317–1322.
Forrez, I., Carballa, M., Noppe, H., Brabander, H.D., Boon, N., Verstraete, W, 2009. Influence of manganese and ammonium oxidation on the removal of 17α-ethinylestradiol (EE2). Water Res. 43 (1), 77–86.
Gaston, L., Lapworth, D.J., Stuart, M., Arnscheidt, J., 2019. Prioritization approaches for substances of emerging concern in groundwater: a critical review. Environ. Sci. Technol. 53, 6107–6122.
Gu, B., Schmitt, J., Chen, Z., Liang, L., McCarthy, J.F., 1994. Adsorption and desorption of natural organic matter on iron oxide: mechanisms and models. Environ. Sci. Technol. 28 (1), 38–46.
Gude, J.C.J., Rietveld, L.C., van Halem, D., 2016. Fate of low arsenic concentrations during full-scale aeration and rapid filtration. Water Res. 88, 566–574.
Hedegaard, M.J., Albrechtsen, H.J., 2014. Microbial pesticide removal in rapid sand filters for drinking water treatment – Potential and kinetics. Water Res. 48 (1), 71–81.
Hedegaard, M.J., Arvin, E., Corfitzen, C.B., Albrechtsen, H.J., 2014. Mecoprop (MCPP) removal in full-scale rapid sand filters at a groundwater-based waterworks. Sci. Total Environ. 499, 257–264.
Ho, L., Meyn, T., Keegan, A., Hoefel, D., Brookes, J., Saint, C.P., Newcombe, G., 2006. Bacterial degradation of microcystin toxins within a biologically active sand filter. Water Res. 40 (4), 768–774.
Hu, W., Liang, J., Ju, F., Wang, Q., Liu, R., Bai, Y., Liu, H., Qu, J., 2020. Metagenomics unravels differential microbiome composition and metabolic potential in rapid sand filters purifying surface water versus groundwater. Environ. Sci. Technol. 54 (8), 5197–5206.
Huguet, M., Deborde, M., Papot, S., Gallard, H., 2013. Oxidative decarboxylation of diclofenac by manganese oxide bed filter. Water Res. 47 (14), 5400–5408.
Huguet, M., Simon, V., Gallard, H., 2014. Transformation of paracetamol into 1,4-benzoquinone by a manganese oxide bed filter. J. Hazard. Mater. 271, 245–251.
Ilton, E.S., Post, J.E., Heaney, P.J., Ling, F.L., Kerisit, S.N., 2016. XPS determination of Mn oxidation states in Mn (hydr)oxides. Appl. Surf. Sci. 366, 475–485.
Khanzada, N.K., Farid, M.U., Kharraz, J.A., Choi, J., Tang, C.Y., Nghiem, L.D., Jang, A., An, A.K., 2020. Removal of organic micropollutants using advanced membrane-based water and wastewater treatment: a review. J. Membr. Sci. 598, 117672.
Kumar, P., Rehab, H., Hegde, K., Brar, S.K., Cledon, M., Kermanshahi-pour, A., Duy, S.V., Sauvé, S., Surampalli, R.Y., 2020. Physical and biological removal of microcystin-LR and other water contaminants in a biofilter using manganese dioxide coated sand and graphene sand composites. Sci. Total Environ. 703, 135052.
Lai, C.H., Chen, C.Y., 2001. Removal of metal ions and humic acid from water by iron-coated filter media. Chemosphere 44 (5), 1177–1184.
Lee, C.O., Boe-Hansen, R., Musovic, S., Smets, B., Albrechtsen, H.J., Binning, P., 2014. Effects of dynamic operating conditions on nitrification in biological rapid sand filters for drinking water treatment. Water Res. 64, 226–236.
Liu, W., Sutton, N.B., Rijnaarts, H.H.M., Langenhoff, A.A.M, 2020. Anaerobic biodegradation of pharmaceutical compounds coupled to dissimilatory manganese (IV) or iron (III) reduction. J. Hazard. Mater. 388, 119361.
Liu, Z., Solliec, M., Papineau, I., Lompe, K.M., Mohseni, M., Bérubé, P.R., Sauvé, S., Barbeau, B., 2022. Elucidating the removal of organic micropollutants on biological ion exchange resins. Sci. Total Environ. 808, 152137.
Mrkajic, N.S., Hama, J.R., Strobel, B.W., Hansen, H.C.B., Rasmussen, L.H., Pedersen, A. K., Christensen, S.C.B., Hedegaard, M.J., 2021. Removal of phytotoxins in filter sand used for drinking water treatment. Water Res. 205, 117610.
Osenbrück, K., Gläser, H.R., Knöller, K., Weise, S.M., Möder, M., Wennrich, R., Schirmer, M., Reinstorf, F., Busch, W., Strauch, G., 2007. Sources and transport of selected organic micropollutants in urban groundwater underlying the city of Halle (Saale), Germany. Water Res. 41 (15), 3259–3270.
Osorio, S.C., Biesheuvel, P.M., Spruijt, E., Dykstra, J.E., van der Wal, A., 2022. Modeling micropollutant removal by nanofiltration and reverse osmosis membranes: considerations and challenges. Water Res. 225, 119130.
Palomino, D., Stoll, S., 2013. Fulvic acids concentration and pH influence on the stability of hematite nanoparticles in aquatic systems. J. Nanopart. Res. 15, 1428.
Papadopoulou, A., Hedegaard, M.J., Dechesne, A., Albrechtsen, H.J., Musovic, S., Smets, B.F., 2019. Methanotrophic contribution to biodegradation of phenoxy acids in cultures enriched from a groundwater-fed rapid sand filter. Appl. Microbiol. Biotechnol. 103 (2), 1007–1019.
Piai, L., Dykstra, J.E., Adishakti, M.G., Blokland, M., Langenhoff, A.A.M., van der Wal, A., 2019. Diffusion of hydrophilic organic micropollutants in granular activated carbon with different pore sizes. Water Res. 162, 518–527.
Poghosyan, L., Koch, H., Frank, J., van Kessel, M.A.H.J., Cremers, G., van Alen, T., Jetten, M.S.M., Op den Camp, H.J.M., Lücker, S., 2020. Metagenomic profiling of ammonia- and methane-oxidizing microorganisms in two sequential rapid sand filters. Water Res. 185, 116288.
Rhodes-Dicker, L., Passesport, E., 2019. Effects of cold-climate environmental factors temperature and salinity on benzotriazole adsorption and desorption in bioretention cells. Ecol. Eng. 127, 58–65.
Singh, S.K., Subramanian, V., Gibbs, R.J., 1984. Hydrous FE and MN oxides — Scavengers of heavy metals in the aquatic environment. Crit. Rev. Environ. Control 14 (1), 33–90.
Sjerps, R.M.A., Kooij, P.J.F., van Loon, A., Van Wezel, A.P., 2019. Occurrence of pesticides in Dutch drinking water sources. Chemosphere 235, 510–518.
Stenkamp, V.S., Benjamin, M.M, 1994. Effect of iron oxide coating on sand filtration. J. Am. Water Works AssOC. 86 (8), 37–50.
Stone, A.T., Morgan, J.J., 1984. Reduction and dissolution of manganese (III) and manganese (IV) oxides by organics. 1. Reaction with hydroquinone. Environ. Sci. Technol. 18 (6), 450–456.
Tan, W., Lu, S., Liu, F., Feng, X., He, J., Koopal, L.K., 2008. Determination of the point-of-zero charge of manganese oxides with different methods including an improved salt titration method. Soil Sci. 173 (4), 277–286.
Tejedor-Tejedor, M.I., Yost, E.C., Anderson, M.A., 1990. Characterization of benzoic and phenolic complexes at the goethite/aqueous solution interface using cylindrical

internal reflection Fourier transform infrared spectroscopy. Part 1. Methodology. Langmuir 6 (5), 979–987.
Vindedahl, A.M., Strehlau, J.H., Arnold, W.A., Penn, R.L., 2016. Organic matter and iron oxide nanoparticles: aggregation, interactions, and reactivity. Environ. Sci. Nano 3, 494–505.
Vries, D., Bertelkamp, C., Schoonenberg Kegel, F., Hofs, B., Dusseldorp, J., Bruins, J.H., de Vet, W., van den Akker, B., 2017. Iron and manganese removal: recent advances in modelling treatment efficiency by rapid sand filtration. Water Res. 109, 35–45.
Wagner, T.V., Parsons, J.R., Rijnaarts, H.H.M., de Voogt, P., Langenhoff, A.A.M., 2020. Benzotriazole removal mechanisms in pilot-scale constructed wetlands treating cooling tower water. J. Hazard. Mater. 384, 121314.
Wang, D., Pan, C., Liu, Z., Chen, K., Chen, N., Liu, S., 2021a. Synergetic effect of two inhibitors for enhanced corrosion protection on the reinforcing steel in the chloride-contaminated carbonated solutions. Constr. Build. Mater. 286, 122916.
Wang, J., de Ridder, D., van der Wal, A., Sutton, N.B., 2021b. Harnessing biodegradation potential of rapid sand filtration for organic micropollutant removal from drinking water: a Review. Crit. Rev. Environ. Sci. Technol. 51 (18), 2086–2118.
Wang, J., Poursat, B.A.J., Feng, J., de Ridder, D., Zhang, C., van der Wal, A., Sutton, N.B., 2022a. Exploring organic micropollutant biodegradation under dynamic substrate loading in rapid sand filters. Water Res. 221, 118832.
Wang, J., Zhang, C., Poursat, B.A.J., de Ridder, D., Smidt, H., van der Wal, A., Sutton, N. B., 2022b. Unravelling the contribution of nitrifying and methanotrophic bacteria to micropollutant co-metabolism in rapid sand filters. J. Hazard. Mater. 424, 127760.
Yamashita, T., Hayes, P., 2008. Analysis of XPS spectra of Fe^{2+} and Fe^{3+} ions in oxide materials. Appl. Surf. Sci. 254 (8), 2441–2449.
Yang, H., Yan, Z., Du, X., Bai, L., Yu, H., Ding, A., Li, G., Liang, H., Aminabhavi, Y.M., 2020. Removal of manganese from groundwater in the ripened sand filtration: biological oxidation versus chemical auto-catalytic oxidation. Chem. Eng. J. 382, 123033.
Yang, K., Yu, J., Guo, Q., Wang, C., Yang, M., Zhang, Y., Xia, P., Zhang, D., Yu, Z., 2017. Comparison of micropollutants' removal performance between pre-ozonation and post-ozonation using a pilot study. Water Res. 111, 147–153.
Yost, E.C., Tejedor-Tejedor, M.I., Anderson, M.A., 1990. *In situ* CIR-FTIR characterization of salicylate complexes at the goethite/aqueous solution interface. Environ. Sci. Technol. 24 (6), 822–828.
Yu, L., Fink, G., Wintgens, T., Melin, T., Ternes, T.A., 2009. Sorption behavior of potential organic wastewater indicators with soils. Water Res. 43, 951–960.
Zearley, T.L., Summers, R.S., 2012. Removal of trace organic micropollutants by drinking water biological filters. Environ. Sci. Technol. 46 (17), 9412–9419.
Zhang, H., Huang, C.H., 2005. Reactivity and transformation of antibacterial *N*-Oxides in the presence of manganese oxide. Environ. Sci. Technol. 39 (2), 593–601.
Zhong, C., Zhao, H., Cao, H., Fu, J., Xie, Y., Sun, Z., 2019. Acidity induced fast transformation of acetaminophen by different MnO_2: kinetics and pathways. Chem. Eng. J. 359, 518–529.
Zuehlke, S., Duennbier, U., Heberer, T., 2007. Investigation of the behavior and metabolism of pharmaceutical residues during purification of contaminated ground water used for drinking water supply. Chemosphere 69 (11), 1673–1680.